# ATLAS NOTE

ATLAS-CONF-2012-105

August 8, 2012

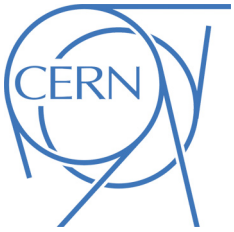


# Search for Supersymmetry in final states with two same-sign leptons, jets and missing transverse momentum with the ATLAS detector in pp collisions at $\sqrt{s} = 8$ TeV

The ATLAS Collaboration

**Abstract**

A search for the production of supersymmetric particles decaying into final states with jets, missing transverse momentum and two isolated leptons, $e$ or $\mu$, of the same sign is presented. The analysis uses a data sample collected during the first half of 2012 that corresponds to a total integrated luminosity of 5.8 fb$^{-1}$ of $\sqrt{s} = 8$ TeV proton-proton collisions recorded with the ATLAS detector at the Large Hadron Collider. No deviation from the Standard Model expectation is observed. Exclusion limits are derived in simplified models in Supersymmetry where the gluino decays via a top squark into $t\bar{t}\,\tilde{\chi}_1^0$. In those models, gluino masses below 800 – 890 GeV are excluded for neutralino masses up to 360 GeV. In the MSUGRA/CMSSM framework with $\tan\beta = 10$, $A_0 = 0$ and $\mu > 0$, $m_{1/2}$ values are excluded below 270 – 420 GeV for $m_0$ values up to 3 TeV.

ATLAS-CONF-2012-105
13 August 2012

# 1 Introduction

Supersymmetry (SUSY) [1–9] predicts new bosonic partners for the fermions and fermionic partners for the bosons in the Standard Model (SM). In $R$-parity conserving SUSY models [10–14], the lightest supersymmetric particle (LSP) is stable and weakly interacting, and SUSY particles are pair-produced in proton-proton collisions. The LSP escapes detection, giving rise to events with significant missing transverse momentum ($\boldsymbol{p}_{\mathrm{T}}^{\mathrm{miss}}$ and its magnitude $E_{\mathrm{T}}^{\mathrm{miss}}$). The dominant production channels for SUSY particles at the LHC are squark-(anti)squark, squark-gluino and gluino pair production, if on-shell squarks and gluinos can be produced with the available beam energies.

In SUSY models, the gluino is a strongly-interacting Majorana fermion. Several SUSY scenarios predict that one of the supersymmetric partners of the top quark ($\tilde{t}_1$) and the anti-top quark ($\tilde{t}_1^*$) are lighter than the other squarks [15, 16]. Therefore top quarks and (virtual) $\tilde{t}_1$ squarks can be produced copiously in gluino decays via $\tilde{g}\tilde{g} \to t\bar{t}\,\tilde{t}_1\tilde{t}_1^*, tt\,\tilde{t}_1^*\tilde{t}_1^*, \bar{t}\bar{t}\,\tilde{t}_1\tilde{t}_1$ [17–21]. The $\tilde{t}_1$ squark can further decay to the lightest chargino ($\tilde{\chi}_1^{\pm}$) or lightest neutralino ($\tilde{\chi}_1^0$) via $\tilde{t}_1 \to b\tilde{\chi}_1^{\pm}$ or $\tilde{t}_1 \to t\,\tilde{\chi}_1^0$ producing isolated leptons and jets in the top quark or chargino decay. A signature for such processes are therefore events with isolated leptons, jets and missing transverse momentum from the undetected neutralinos. Pair-produced gluinos have equal probability to produce in their decays a pair of leptons with the same charge (same-sign, SS) and opposite charge (opposite-sign, OS).

This analysis considers events with pairs of isolated same-sign leptons $\ell\ell$ ($ee$, $e\mu$, $\mu\mu$), multiple high-$p_{\mathrm{T}}$ jets and large $E_{\mathrm{T}}^{\mathrm{miss}}$. The requirement of SS leptons utilizes the Majorana nature of the gluino and suppresses the contribution from SM processes and thus enhances the potential SUSY signal significance. The main background arises from Standard Model processes (mainly $t\bar{t}$) with one isolated lepton and another reconstructed lepton from heavy flavor decays (HF fakes). Smaller background contributions are expected from $t\bar{t}+W/Z$, isolated lepton pairs where the sign of one lepton charge is wrongly reconstructed (charge mis-ID, mainly from $Z/\gamma^*, t\bar{t}$) and real SS dilepton events from $WZ$ and $ZZ$ processes (diboson). This note presents a search for SUSY in events with SS dileptons at $\sqrt{s} = 8$ TeV. Previous results have been published by ATLAS at $\sqrt{s} = 7$ TeV [22] and CMS at $\sqrt{s} = 7$ TeV [23] and 8 TeV [24].

# 2 ATLAS detector and event reconstruction

The ATLAS detector [25] features tracking detectors surrounded by a 2 T superconducting solenoid, calorimeters, and a muon spectrometer in a toroidal magnetic field. The calorimeters, with acceptance covering the pseudorapidity range $|\eta| < 4.9$, are composed of high-granularity liquid-argon calorimeters with lead, copper, or tungsten absorbers and an iron scintillator calorimeter.

Jets are reconstructed from three-dimensional calorimeter energy clusters by using the anti-$k_t$ algorithm [26,27] with a radius parameter of 0.4. Jet energies are corrected [28] for detector inhomogeneities, the non-compensating nature of the calorimeter, and the impact of multiple overlapping $pp$ interactions, using factors derived from test beam, cosmic ray, $pp$ collision data and from a detailed Geant4 [29] detector simulation [30]. Jets are required to have $p_{\mathrm{T}} > 20$ GeV and $|\eta| < 2.8$.

Electron candidates must satisfy the "tight" selection criteria as defined in Ref. [31] and are required to fullfill $p_{\mathrm{T}} > 20$ GeV, $|\eta| < 2.47$ and to be isolated, i.e. the scalar sum of $p_{\mathrm{T}}$ of charged tracks, $\Sigma p_{\mathrm{T}}$, within a cone in the $\eta - \phi$ plane of radius $\Delta R = 0.2$ around the candidate excluding its own track must be less than 10% of the electron $p_{\mathrm{T}}$. They must have longitudinal and transverse impact parameters within 2 mm and 1 mm, respectively, of the primary vertex. Muon candidates are required to have $p_{\mathrm{T}} > 20$ GeV, $|\eta| < 2.4$ and are identified by matching an extrapolated inner detector track and one or more track segments in the muon spectrometer [32, 33]. In addition, muons are required to have longitudinal and transverse impact parameters within 1 mm and 0.2 mm, respectively, of the primary vertex and to be isolated, i.e. $\Sigma p_{\mathrm{T}} < 1.8$ GeV for a cone with $\Delta R = 0.2$.

The calculation of $E_{\mathrm{T}}^{\mathrm{miss}}$ [34] is based on the vectorial sum of the $p_{\mathrm{T}}$ of reconstructed jets (with $p_{\mathrm{T}} >$ 20 GeV and $|\eta| < 4.5$) and leptons as well as calorimeter energy clusters not belonging to reconstructed objects.

# 3 Monte Carlo Simulation

Simulated Monte Carlo events are used to model the SUSY signal efficiency, to optimize the event selection requirements and to aid in the description of the Standard Model backgrounds. Top-quark pair and single-top production are simulated with MC@NLO [35], fixing the top-quark mass at 172.5GeV, and using the next-to-leading-order (NLO) parton density function (PDF) set CT10 [36]. Samples of $W$+jets and $Z$+jets with both light- and heavy-flavor jets are generated with ALPGEN [37] and PDF set CTEQ6L1 [38]. The fragmentation and hadronization for the ALPGEN and MC@NLO samples are performed with HERWIG [39], using JIMMY [40] for the underlying event. Samples of $t\bar{t}\,W$(+jets) and $t\bar{t}\,Z$ (+jets), referred to as $t\bar{t}+V$, are generated with MADGRAPH [41] interfaced to PYTHIA [42]. The total LO cross sections for these samples are 0.197 pb and 0.155 pb, respectively. They are normalized to NLO using K-factors of 1.2 and 1.3 for $t\bar{t}\,W$ and $t\bar{t}\,Z$, respectively [43–45]. Diboson samples are generated with SHERPA and PDF set CT10 for $WW$, $WZ$ and $ZZ$ processes and normalized to NLO cross sections with K-factors of 1.07, 1.06 and 1.11, respectively [46, 47]. SUSY signal processes are simulated using HERWIG++. The MSUGRA/CMSSM [48–53] particle spectrum is calculated with SOFTSUSY [54] using $\tan\beta = 10$, $A_0 = 0$ and $\mu > 0$. The SUSY sample yields are normalized to the results of next-to-leading order calculations in $\alpha_s$, including the resummation of soft gluon emission at next-to-leading-logarithmic accuracy (NLO+NLL) [55–59].

The nominal cross sections and the uncertainties are taken from an envelope of cross section predictions using different PDF sets and factorization and renormalization scales, as described in Ref. [60]. This results in theoretical uncertainties of 30% and 50% for the $t\bar{t}W$ and $t\bar{t}Z$ and 10% for $t\bar{t}$ cross sections, respectively. The theoretical uncertainties of SUSY signal processes depend on the parameter choices; they are typically around 25%.

MC samples are processed through a detector simulation [30] based on Geant4 [29] and reconstructed in the same manner as the data. The simulation includes the effect of multiple $pp$ collisions and is weighted to reproduce the observed distribution of the average number of collisions per bunch crossing.

# 4 Event selection and background

The data set corresponds to a total integrated luminosity of 5.8 fb$^{-1}$ with a relative uncertainty of 3.6% of proton proton collision data at $\sqrt{s} = 8$ TeV taken in the first half of 2012. This data set is selected by a three-level trigger system. The signal region selection is based on an $E_{\mathrm{T}}^{\mathrm{miss}}$ trigger, which provides an efficiency in excess of 97% for $E_{\mathrm{T}}^{\mathrm{miss}} > 150$ GeV. For background and validation studies, dilepton triggers are used to define a control sample with $E_{\mathrm{T}}^{\mathrm{miss}} < 150$ GeV.

Events in which the two highest $p_{\mathrm{T}}$ electrons or muons with $p_{\mathrm{T}} > 20$ GeV have the same electric charge are preselected. In addition, at least four jets with $p_{\mathrm{T}} > 50$ GeV are required. The lepton and high $p_{\mathrm{T}}$ jet requirements lead to a reduced sensitivity to pile-up effects. On top of these baseline requirements the signal region is defined by $E_{\mathrm{T}}^{\mathrm{miss}} > 150$ GeV. The requirement for the signal region was optimized with various models of gluino decays with isolated same-sign leptons in the final state [22].

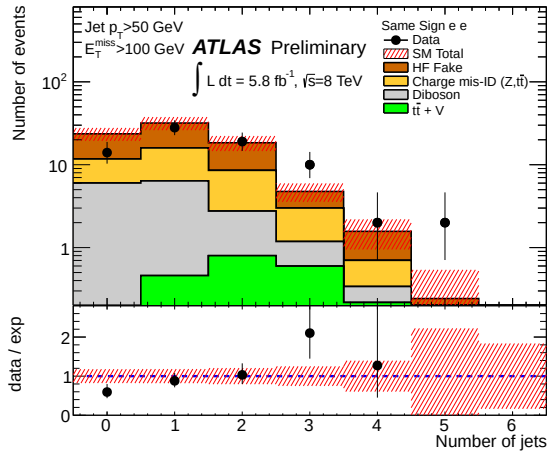


(a) Number of jets in the $ee$ channel.

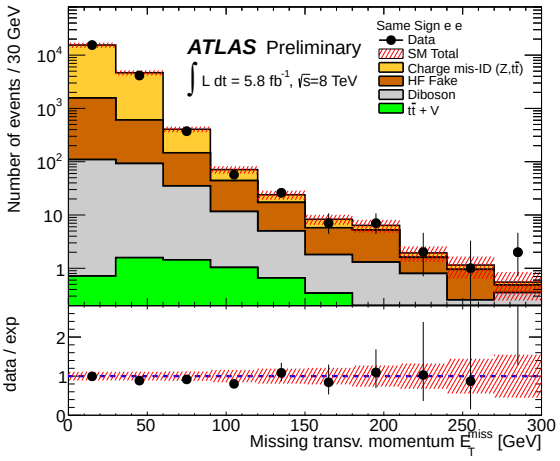


(b) $E_{\mathrm{T}}^{\mathrm{miss}}$ in the $ee$ channel.

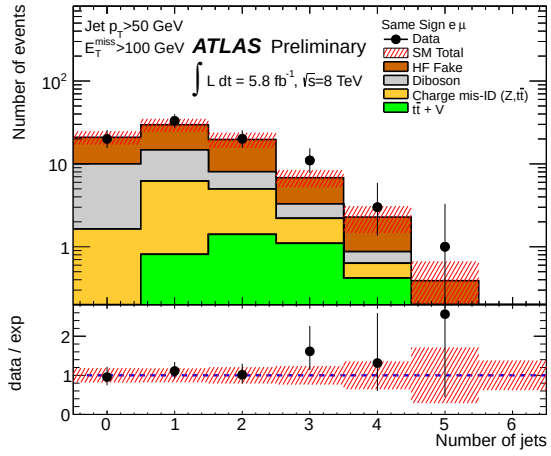


(c) Number of jets in the $e\mu$ channel.

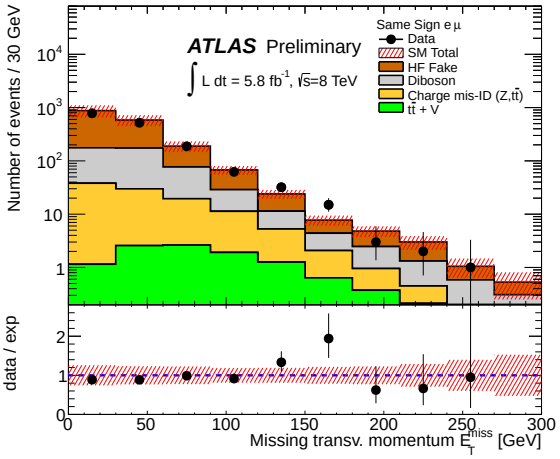


(d) $E_{\mathrm{T}}^{\mathrm{miss}}$ in the $e\mu$ channel.

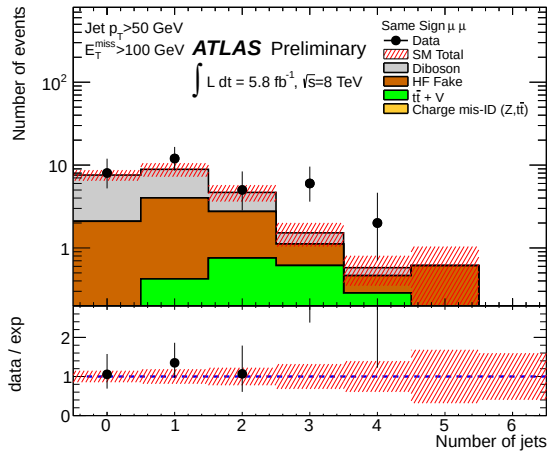


(e) Number of jets in the $\mu\mu$ channel.

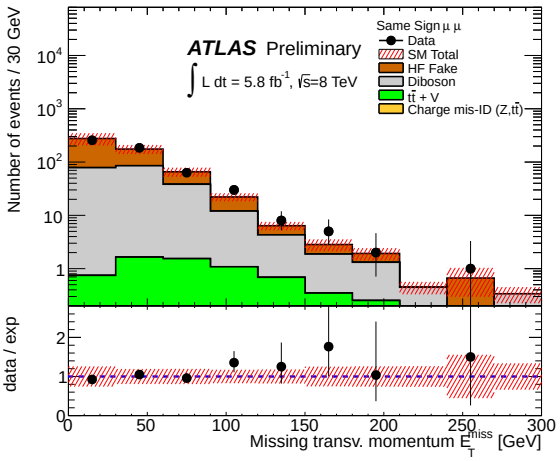


(f) $E_{\mathrm{T}}^{\mathrm{miss}}$ in the $\mu\mu$ channel.

Figure 1: The left plots show the number of jets with $p_{\mathrm{T}} > 50$ GeV for SS dilepton events with $E_{\mathrm{T}}^{\mathrm{miss}} > 100$ GeV. On the right the $E_{\mathrm{T}}^{\mathrm{miss}}$ distributions for preselected SS dilepton events are displayed. The data points are compared with the sum of the expected contributions from HF fakes, real SS dileptons from diboson and $t\bar{t}+V$ as well as charge mis-identification from $t\bar{t}$ or $Z$+jets events. Charge mis-identification has a negligible impact on muons. The red-shaded error band around the expectation contains Monte Carlo statistics, jet energy scale systematics and the uncertainty of the HF estimate.

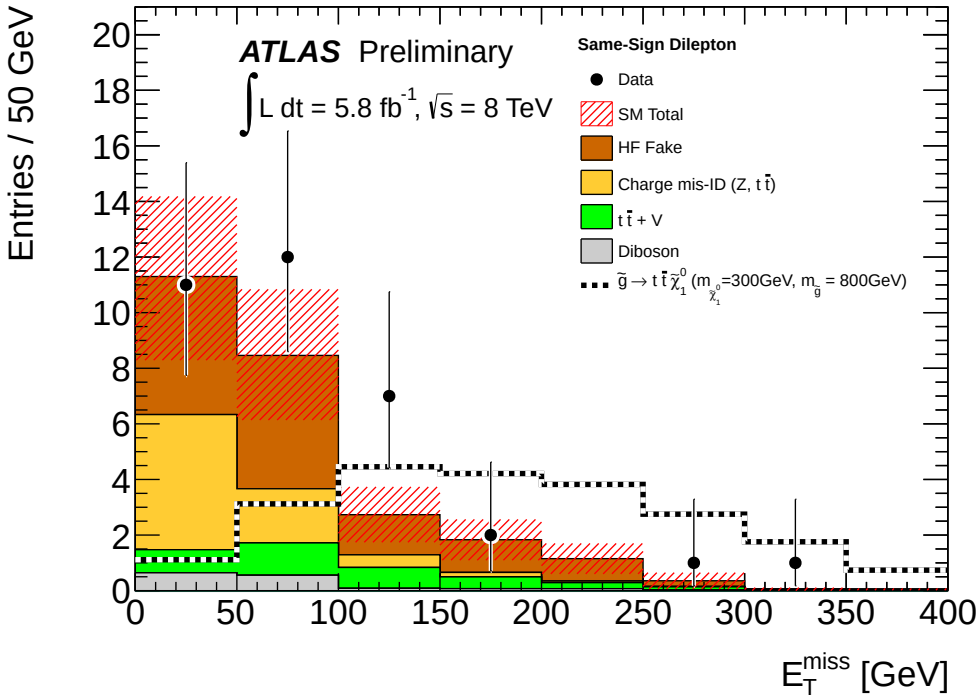


Figure 2: Distribution of $E_{\mathrm{T}}^{\mathrm{miss}}$ for dilepton events with the baseline selection. The data points are compared with the sum of the expected contribution from HF fakes, real SS dileptons from diboson and $t\bar{t}+V$ as well as charge mis-identification from $t\bar{t}$ or $Z$+jets events. The red-shaded error band around the expectation contains all statistical and systematical uncertainties of the background prediction.

The SM backgrounds are evaluated using a combination of Monte Carlo simulations and data driven techniques. Three main classes of backgrounds can be distinguished: real SS lepton pairs, fake leptons and charge mis-identifications. The contribution of real SS lepton pairs from diboson and $t\bar{t}+V$ processes to the signal region are estimated using Monte Carlo simulations.

The fake lepton background, which is dominant for all flavor channels, arises from events with jets which are mis-identified as leptons or with semi-leptonically decaying hadrons containing heavy flavor $c$- or $b$-quarks (HF fake). The main contribution is expected from semi-leptonic $t\bar{t}$ events with a fake lepton from $b$-decays. This background is estimated from the data using the same method as in [22] by loosening the lepton identification and isolation criteria, yielding classes of "tight" and "loose" leptons. The method counts the number of observed events containing loose-loose, loose-tight, tight-loose and tight-tight lepton pairs. Using four linear equations, the number of events in the signal region with fake-fake, fake-real, real-fake and real-real lepton pairs can be determined. The parameters of the equations contain two types of probabilities for electrons and muons separately: the probability for a loose fake lepton and the probability for a loose real lepton to pass the tight selection criteria. These probabilities are measured as a function of the lepton $p_{\mathrm{T}}$ and pseudorapidity $\eta$ from data. The real lepton probabilities are determined from a data sample enriched with real leptons from $Z \to \ell^+\ell^-$ decays, obtained by requiring 80 GeV $< m_{\ell\ell} <$ 100 GeV. The fake lepton probabilities are measured from a data set enriched with one real muon and an additional fake lepton. The electron fake rate is determined from a sample of SS $e\mu$ events with at least one tagged $b$-jet and a muon with $p_{\mathrm{T}} > 40$ GeV passing tight selection cuts, whereas the electron must have 20 GeV $< p_{\mathrm{T}} <$ 40 GeV. The muon fake rate is determined from a sample of SS dimuon events with 20 GeV $< p_{\mathrm{T}} <$ 40 GeV, where at least one of them is required to pass the tight

| Category | $ee$ | $e\mu$ | $\mu\mu$ | $\ell\ell$ |
|---|---|---|---|---|
| HF fake | $0.74 \pm 0.53$ | $1.16 \pm 0.70$ | $0.25^{+0.30}_{-0.25}$ | $2.14 \pm 1.08$ |
| $t\bar{t} + V$ | $0.17 \pm 0.08$ | $0.44 \pm 0.18$ | $0.23 \pm 0.10$ | $0.84 \pm 0.34$ |
| Charge mis-ID ($Z$,$t\bar{t}$) | $0.13 \pm 0.06$ | $0.14 \pm 0.06$ | – | $0.27 \pm 0.10$ |
| Diboson | $0.04 \pm 0.04$ | $0.10 \pm 0.05$ | $0.03 \pm 0.03$ | $0.18 \pm 0.07$ |
| Total background | $1.1 \pm 0.5$ | $1.8 \pm 0.7$ | $0.5 \pm 0.3$ | $3.4 \pm 1.1$ |
| Observed in data | 1 | 2 | 1 | 4 |

Table 1: Number of observed SS dilepton events in the data in the signal region together with the expected SM background events. The errors include the total statistical and systematic uncertainties. Category $\ell\ell$ denotes the sum of all dilepton classes.

selection criteria. The $p_{\mathrm{T}}$ range was chosen in order to enhance the fraction of fake leptons in the control sample. The extrapolation to the $p_{\mathrm{T}} > 40\,\mathrm{GeV}$ validation region has been tested by several methods and the differences of the results have been assigned as systematic uncertainty.

Background events from charge misidentification are dominated by electrons which have undergone hard bremsstrahlung with subsequent photon conversion. They are estimated using a partially data-driven technique [61]. The probability of lepton charge misidentification is determined in the data using the ratio of SS to OS electron pairs with an invariant mass compatible with the Z boson within 15 GeV. This probability is applied to MC simulations of $t\bar{t}$ and $Z$+jets events in order to determine the background contribution of these processes in the signal region. The probability of misidentifying the charge of a muon is negligible.

Using the above methods, good agreement is observed between data and the predicted Standard Model background. This is demonstrated in the following validation regions, which are chosen to be supersets of the signal region and to have high event yields from SM sources. Figure 1 (left column) shows the distribution of the number of jets of $p_{\mathrm{T}} > 50$ GeV for events with $E_{\mathrm{T}}^{\mathrm{miss}} > 100$ GeV. The data points are compared with the sum of the expected contribution from HF fakes, real SS dileptons from diboson and $t\bar{t} + V$ as well as charge mis-identification from $t\bar{t}$ or $Z$+jets events. Similarly, Figure 1 (right column) shows the $E_{\mathrm{T}}^{\mathrm{miss}}$ distribution for preselected SS dilepton events (no jet requirements applied) compared to the same background sources. Figure 2 shows the combined $E_{\mathrm{T}}^{\mathrm{miss}}$ distribution for all SS leptons ($ee$, $e\mu$, $\mu\mu$) after baseline requirements.

# 5 Results

The number of expected events and the uncertainty for each background source in the signal region is given in Table 1. In total 4 events are observed in the signal region with $E_{\mathrm{T}}^{\mathrm{miss}} > 150\,\mathrm{GeV}$. One event each is observed in the $ee$ and $\mu\mu$ channels, and 2 events in the $e\mu$ channel. The largest background contributions are expected from fake leptons from heavy flavor (mainly from $b$-jets in $t\bar{t}$ decays) and $t\bar{t}$ production with an additional $W$ or $Z$ vector boson. Smaller background contributions are expected from $t\bar{t}$ and $Z$ decays where one of the leptons has a charge mis-identification.

The dominant source of systematic uncertainties in the background estimation is attributed to HF fake leptons. They arise mainly from the statistical error of the data sample used to estimate the fake rate and from the systematic uncertainties to transfer the estimate from the control to the signal region. The uncertainties of the contributions from the remaining background categories (arising mainly from

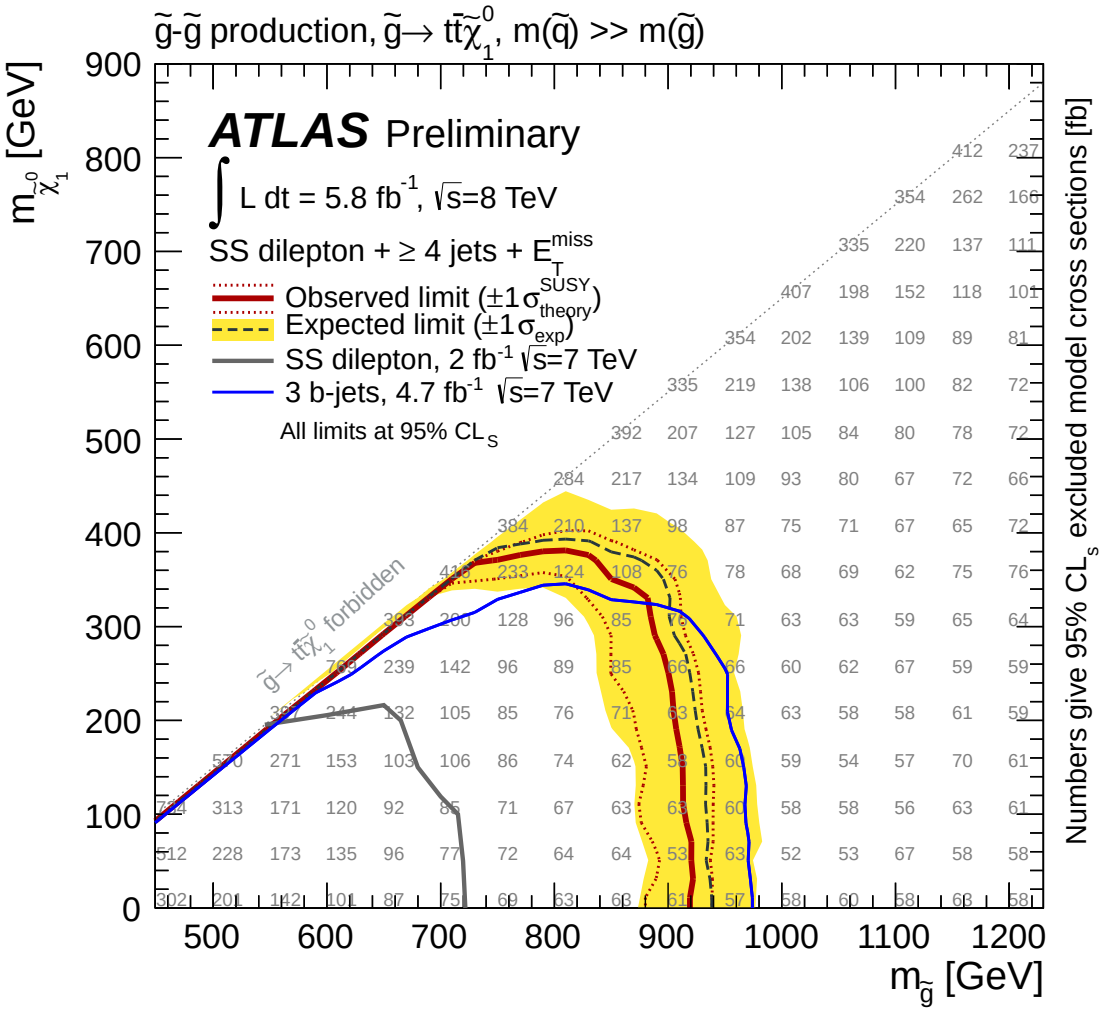


Figure 3: Expected and observed 95% C.L. limits for a $\tilde{g} \to t\bar{t}\,\tilde{\chi}_1^0$ decay model in a plane of the gluino and neutralino masses. The numbers give the limits on the excluded model cross sections. Uncertainties due to the signal cross-section are indicated by the red dashed lines around the observed limit. All other systematics (detector-related, background estimation) are indicated by the yellow band around the expected limit. Also indicated are previous ATLAS limits using 7 TeV data.

MC statistics, jet energy scale and theory uncertainties) have a minor effect on the total background uncertainty.

Since the total number of observed events (4) agrees with the Standard Model expectation ($3.4 \pm 1.1$) the measurement is used to place limits on the production of SUSY particles. The results are interpreted as exclusion limits for a *CLs* likelihood ratio combining Poisson probabilities for signal and background [62]. From the observation, a model independent 95% C.L. upper limit can be placed on the visible cross section $\sigma_{\rm vis} = \sigma \times$ efficiency $< 1.08$ fb in the signal region. This corresponds to a 95% C.L. observed upper limit of 6.3 signal events, compared to an expected upper limit of $5.7^{+2.0}_{-1.1}$ events. The confidence level for the background-only hypothesis is 65%.

The measurement is also used to place limits for a simplified model in which the gluino decays via

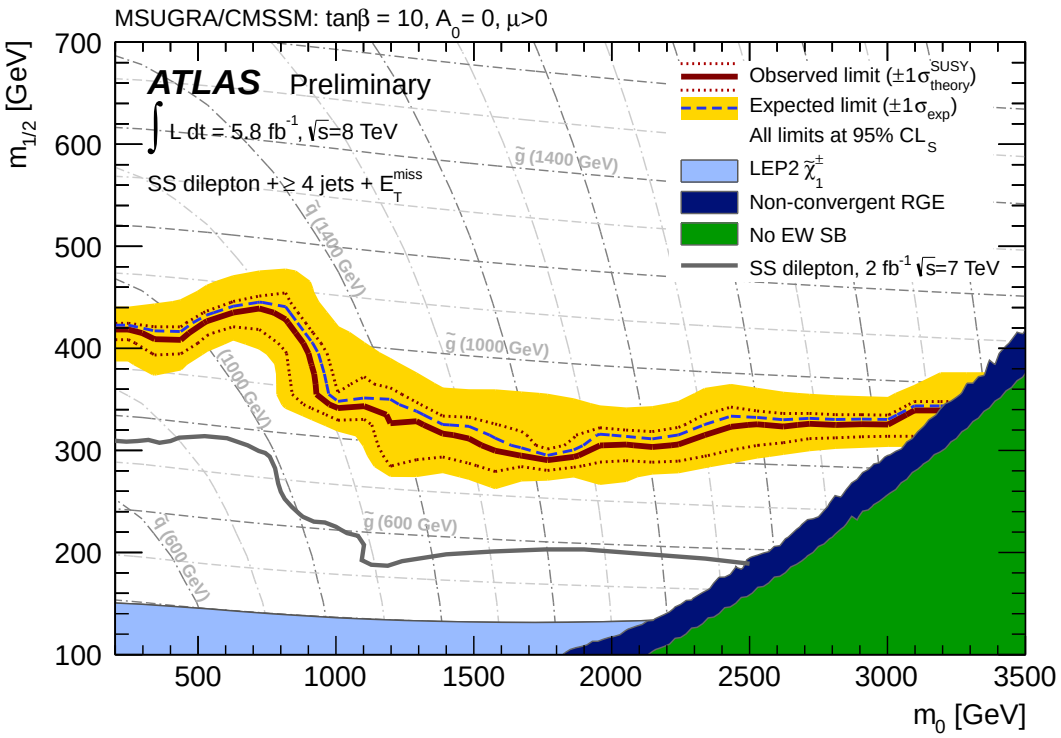


Figure 4: Expected and observed 95% C.L. limits in a MSUGRA/CMSSM model for the search in the same sign lepton channel at $\sqrt{s} = 8$ TeV. The limits are compared to the previous ATLAS results, which use 7 TeV data. Uncertainties on signal cross-section are given by the red dashed lines. All other systematics (detector-related, background estimation) are indicated by the yellow band around the expected limit. Regions excluded by theoretical considerations include the absence of electroweak symmetry breaking due to wrong Higgs parameter sign (green), and the non-convergence of numerical algorithms solving the renormalization group equations (dark blue).

an off-shell top squark into $t\bar{t}$+neutralino ($\tilde{g} \rightarrow t\tilde{t}_1 \rightarrow t\bar{t}\,\tilde{\chi}_1^0$) using $m_{\tilde{t}} = 2.5$ TeV [1] and assuming much higher masses for other squarks. The exclusion limits (95% C.L.) in the $m_{\tilde{g}}$ vs. $m_{\tilde{\chi}_1^0}$ plane are displayed in Figure 3, enlarging significantly the exclusion region of previous ATLAS results, which are based on a subset of 2011 7 TeV data [22]. For comparison, the observed ATLAS limits from a search based on final states with three $b$-jets and missing transverse energy [63] are also indicated. With this analysis gluinos can be excluded with 95% C.L. up to masses of 800 – 890 GeV for neutralino masses below 360 GeV, these values are derived from the $-1\sigma$ observed limit contour to account for theoretical uncertainties on the SUSY cross sections.

In MSUGRA/CMSSM SUSY models the main source of same-sign leptons are gluino decays involving charginos and neutralinos. At high $m_0$ values, gluino pair production is dominant and the most important decay mode for SS leptons is $\tilde{g} \rightarrow \tilde{\chi}_1^{\pm} jj$, where the chargino decays subsequently into leptons. Another important decay mode is $\tilde{g} \rightarrow \tilde{\chi}_2^0 jj$ followed by $\tilde{\chi}_2^0 \rightarrow \ell^+\ell^-\tilde{\chi}_1^0$. Figure 4 shows the exclusion limits for an MSUGRA/CMSSM model with $\tan\beta = 10$, $A_0 = 0$ and $\mu > 0$. Values for $m_{1/2}$ below 270 – 420 GeV are excluded for $m_0 < 3$ TeV. This results in excluding gluino masses below 800 GeV for any squark mass. The limit increases up to gluino masses of 1 TeV for squark masses below 1.2 TeV.

[1] The results are insensitive to the choice of the off-shell top squark mass as long as $m_{\tilde{q}} \gg m_{\tilde{g}}$ and the decay length of the gluino is much smaller than 1 mm.

# 6 Conclusion

Results of a search are presented for the production of supersymmetric particles decaying into final states with jets, missing transverse momentum and two isolated leptons, e or $\mu$, of the same sign. The analysis uses a data sample collected during the first half of 2012 that corresponds to a total integrated luminosity of 5.8 fb$^{-1}$ of $\sqrt{s} = 8$ TeV proton-proton collisions recorded with the ATLAS detector at the Large Hadron Collider. No deviation from the Standard Model expectation is observed. Exclusion limits are derived in simplified SUSY models where the gluino decays into a pair of top squarks and missing energy as well as in the MSUGRA/CMSSM framework. In those simplified models, gluino masses below $800 - 890$ GeV are excluded for LSP masses up to 360 GeV. In the MSUGRA/CMSSM framework with $\tan\beta = 10$, $A_0 = 0$ and $\mu > 0$, values for $m_{1/2}$ are excluded below $270 - 420$ GeV for the for $m_0 < 3$ TeV. In this model gluinos of mass $< 800$ GeV are excluded and a limit of 1 TeV is observed for squark masses below 1.2 TeV. This measurement significantly improves previous limits, which were based on a subset of the 7 TeV ATLAS data.

## References


[1] H. Miyazawa, *Baryon Number Changing Currents*, Prog. Theor. Phys. **36 (6)** (1966) 1266–1276.

[2] P. Ramond, *Dual Theory for Free Fermions*, Phys. Rev. **D3** (1971) 2415–2418.

[3] Y. A. Golfand and E. P. Likhtman, *Extension of the Algebra of Poincare Group Generators and Violation of p Invariance*, JETP Lett. **13** (1971) 323–326. [Pisma Zh.Eksp.Teor.Fiz.13:452-455,1971].

[4] A. Neveu and J. H. Schwarz, *Factorizable dual model of pions*, Nucl. Phys. **B31** (1971) 86–112.

[5] A. Neveu and J. H. Schwarz, *Quark Model of Dual Pions*, Phys. Rev. **D4** (1971) 1109–1111.

[6] J. Gervais and B. Sakita, *Field theory interpretation of supergauges in dual models*, Nucl. Phys. **B34** (1971) 632–639.

[7] D. V. Volkov and V. P. Akulov, *Is the Neutrino a Goldstone Particle?*, Phys. Lett. **B46** (1973) 109–110.

[8] J. Wess and B. Zumino, *A Lagrangian Model Invariant Under Supergauge Transformations*, Phys. Lett. **B49** (1974) 52.

[9] J. Wess and B. Zumino, *Supergauge Transformations in Four-Dimensions*, Nucl. Phys. **B70** (1974) 39–50.

[10] P. Fayet, *Supersymmetry and Weak, Electromagnetic and Strong Interactions*, Phys. Lett. **B64** (1976) 159.

[11] P. Fayet, *Spontaneously Broken Supersymmetric Theories of Weak, Electromagnetic and Strong Interactions*, Phys. Lett. **B69** (1977) 489.

[12] G. R. Farrar and P. Fayet, *Phenomenology of the Production, Decay, and Detection of New Hadronic States Associated with Supersymmetry*, Phys. Lett. **B76** (1978) 575–579.

[13] P. Fayet, *Relations Between the Masses of the Superpartners of Leptons and Quarks, the Goldstino Couplings and the Neutral Currents*, Phys. Lett. **B84** (1979) 416.

[14] S. Dimopoulos and H. Georgi, *Softly Broken Supersymmetry and SU(5)*, Nucl. Phys. **B193** (1981) 150.

[15] R. Barbieri and G. Giudice, *Upper Bounds on Supersymmetric Particle Masses*, Nucl. Phys. **B306** (1988) 63.

[16] B. de Carlos and J. Casas, *One loop analysis of the electroweak breaking in supersymmetric models and the fine tuning problem*, Phys. Lett. **B309** (1993) 320–328, `arXiv:hep-ph/9303291 [hep-ph]`.

[17] W. Beenakker, R. Hopker, T. Plehn, and P. Zerwas, *Stop decays in SUSY-QCD*, Z. Phys. **C75** (1997) 349.

[18] J. Hisano, K. Kawagoe, and M. M. Nojiri, *Detailed study of gluino decay into third generation squarks at the CERN LHC*, Phys. Rev. **D68** (2003) 035007.

[19] C. Balázs, M. Carena, and C. Wagner, *Dark matter, light top squarks, and electroweak baryogenesis*, Phys. Rev. **D70** (2004) 015007.

[20] M. Mühlleitner, A. Djouadi, and Y. Mambrini, *SDECAY: A Fortran code for the decays of the supersymmetric particles in the MSSM*, Comp. Phys. Comm. **168** (2005) 46.

[21] S. Kraml and A. Raklev, *Same-sign top quarks as signature of light stops at the CERN LHC*, Phys. Rev. **D73** (2006) 075002.

[22] ATLAS Collaboration, *Search for gluinos in events with two same-sign leptons, jets and missing transverse momentum with the ATLAS detector in pp collisions at* $\sqrt{s}$ *= 7 TeV*, Phys. Rev. Lett. (2012) 241802, arXiv:1203.5763 [hep-ex].

[23] CMS Collaboration, *Search for new physics with same-sign isolated dilepton events with jets and missing transverse energy*, arXiv:1205.6615 [hep-ex].

[24] CMS Collaboration, *Search for new physics in events with same-sign dileptons and b-tagged jets in pp collisions at* $\sqrt{s}$ *= 8 TeV*, CMS-PAS-SUS-12-017 (2012) .

[25] ATLAS Collaboration, *The ATLAS Experiment at the CERN Large Hadron Collider*, JINST **3** (2008) S08003.

[26] M. Cacciari, G. P. Salam, and G. Soyez, *The anti-$k_t$ jet clustering algorithm*, JHEP **04** (2008) 063, arXiv:0802.1189 [hep-ph].

[27] M. Cacciari and G. P. Salam, *Dispelling the $N^3$ myth for the $k_t$ jet-finder*, Phys. Lett. **B641** (2006) 57–61, arXiv:hep-ph/0512210.

[28] ATLAS Collaboration, *Jet energy measurement with the ATLAS detector in proton-proton collisions at sqrt(s) = 7 TeV*, submitted to Eur. Phys. J. C , arXiv:1112.6426 [hep-ex].

[29] S. Agostinelli et al., *GEANT4: A simulation toolkit*, Nucl. Instrum. Meth. **A506** (2003) 250–303.

[30] ATLAS Collaboration, *The ATLAS Simulation Infrastructure*, Eur. Phys. J. **C70** (2010) 823–874, arXiv:1005.4568 [physics.ins-det].

[31] ATLAS Collaboration, *Electron performance measurements with the ATLAS detector using the 2010 LHC proton-proton collision data*, Eur. Phys. J. **C72** (2012) 1909, arXiv:1110.3174 [hep-ex].

[32] ATLAS Collaboration, *Muon reconstruction efficiency in reprocessed 2010 LHC proton-proton collision data recorded with the ATLAS detector*, ATLAS-CONF-2011-063. https://cdsweb.cern.ch/record/1345743.

[33] ATLAS Collaboration, *A measurement of the ATLAS muon reconstruction and trigger efficiency using J/psi decays*, ATLAS-CONF-2011-021. https://cdsweb.cern.ch/record/1336750.

[34] ATLAS Collaboration, *Performance of Missing Transverse Momentum Reconstruction in Proton-Proton Collisions at 7 TeV with ATLAS*, Eur. Phys. J. **C72** (2012) 1844, arXiv:1108.5602 [hep-ex].

[35] Frixione, Stefano and Webber, Bryan R., *Matching NLO QCD computations and parton shower simulations*, JHEP **06** (2002) 029, arXiv:hep-ph/0204244.

[36] H.-L. Lai, M. Guzzi, J. Huston, Z. Li, P. M. Nadolsky, et al., *New parton distributions for collider physics*, Phys. Rev. **D82** (2010) 074024, arXiv:1007.2241 [hep-ph].

[37] Mangano, M. L. and Moretti, M. and Piccinini, F. and Pittau, R. and Polosa, A. D., *ALPGEN, a generator for hard multiparton processes in hadronic collisions*, JHEP **0307** (2003) 001, arXiv:hep-ph/0206293 [hep-ph].

[38] P. M. Nadolsky, H.-L. Lai, Q.-H. Cao, J. Huston, J. Pumplin, et al., *Implications of CTEQ global analysis for collider observables*, Phys. Rev. **D78** (2008) 013004, arXiv:0802.0007 [hep-ph].

[39] G. Corcella, I. Knowles, G. Marchesini, S. Moretti, K. Odagiri, et al., *HERWIG 6: An Event generator for hadron emission reactions with interfering gluons (including supersymmetric processes)*, JHEP **0101** (2001) 010, arXiv:hep-ph/0011363 [hep-ph].

[40] J. Butterworth, J. R. Forshaw, and M. Seymour, *Multiparton interactions in photoproduction at HERA*, Z.Phys. **C72** (1996) 637–646, arXiv:hep-ph/9601371 [hep-ph].

[41] J. Alwall et al., *MadGraph/MadEvent v4: The New Web Generation*, JHEP **09** (2007) 028, arXiv:0706.2334 [hep-ph].

[42] T. Sjöstrand, S. Mrenna, and P. Z. Skands, *PYTHIA 6.4 Physics and Manual*, JHEP **0605** (2006) 026, arXiv:hep-ph/0603175.

[43] A. Lazopoulos, T. McElmurry, K. Melnikov, and F. Petriello, *Next-to-leading order QCD corrections to $t\bar{t}Z$ production at the LHC*, Phys. Lett. **B666** (2008) 62–65, arXiv:0804.2220 [hep-ph].

[44] J. M. Campbell and R. K. Ellis, *$t\bar{t}W^{\pm}$ production and decay at NLO*, arXiv:1204.5678 [hep-ph].

[45] M. V. Garzelli, A. Kardos, C. G. Papadopoulos, and Z. Trócsányi, *$Z^0$-boson production in association with a $t\bar{t}$ pair at next-to-leading order accuracy with parton shower effects*, Phys. Rev. **D85** (2012) 074022.

[46] J. M. Campbell and R. K. Ellis, *An Update on vector boson pair production at hadron colliders*, Phys. Rev. **D60** (1999) 113006, arXiv:hep-ph/9905386 [hep-ph].

[47] J. M. Campbell, R. K. Ellis, and C. Williams, *Vector boson pair production at the LHC*, JHEP **1107** (2011) 018, arXiv:1105.0020 [hep-ph].

[48] A. H. Chamseddine, R. L. Arnowitt, and P. Nath, *Locally Supersymmetric Grand Unification*, Phys. Rev. Lett. **49** (1982) 970.

[49] R. Barbieri, S. Ferrara, and C. A. Savoy, *Gauge Models with Spontaneously Broken Local Supersymmetry*, Phys. Lett. **B119** (1982) 343.

[50] L. E. Ibanez, *Locally Supersymmetric SU(5) Grand Unification*, Phys. Lett. **B118** (1982) 73.

[51] L. J. Hall, J. D. Lykken, and S. Weinberg, *Supergravity as the Messenger of Supersymmetry Breaking*, Phys. Rev. **D27** (1983) 2359–2378.

[52] N. Ohta, *Grand Unified Theories Based on Local Supersymmetry*, Prog. Theor. Phys. **70** (1983) 542.

[53] G. L. Kane, C. F. Kolda, L. Roszkowski, and J. D. Wells, *Study of constrained minimal supersymmetry*, Phys. Rev. **D49** (1994) 6173–6210, arXiv:hep-ph/9312272 [hep-ph].

[54] B. Allanach, *SOFTSUSY: a program for calculating supersymmetric spectra*, Comput. Phys. Commun. **143** (2002) 305–331, arXiv:hep-ph/0104145 [hep-ph].

[55] W. Beenakker, R. Hopker, M. Spira, and P. Zerwas, *Squark and gluino production at hadron colliders*, Nucl. Phys. **B492** (1997) 51–103, arXiv:hep-ph/9610490 [hep-ph].

[56] A. Kulesza and L. Motyka, *Threshold resummation for squark-antisquark and gluino-pair production at the LHC*, Phys. Rev. Lett. **102** (2009) 111802, arXiv:0807.2405 [hep-ph].

[57] A. Kulesza and L. Motyka, *Soft gluon resummation for the production of gluino-gluino and squark-antisquark pairs at the LHC*, Phys. Rev. **D80** (2009) 095004, arXiv:0905.4749 [hep-ph].

[58] W. Beenakker, S. Brensing, M. Kramer, A. Kulesza, E. Laenen, et al., *Soft-gluon resummation for squark and gluino hadroproduction*, JHEP **0912** (2009) 041, arXiv:0909.4418 [hep-ph].

[59] W. Beenakker, S. Brensing, M. Kramer, A. Kulesza, E. Laenen, et al., *Squark and Gluino Hadroproduction*, Int. J. Mod. Phys. **A26** (2011) 2637–2664, arXiv:1105.1110 [hep-ph].

[60] M. Krämer, A. Kulesza, R. van der Leeuw, M. Mangano, S. Padhi, et al., *Supersymmetry production cross sections in pp collisions at sqrts = 7 TeV*, arXiv:1206.2892 [hep-ph].

[61] ATLAS Collaboration, *Searches for supersymmetry with the ATLAS detector using final states with two leptons and missing transverse momentum in sqrts = 7 TeV proton-proton collisions*, Phys. Lett. **B709** (2012) 137–157, arXiv:1110.6189 [hep-ex].

[62] A. L. Read, *Presentation of search results: The CL(s) technique*, J. Phys. G **G28** (2002) 2693–2704.

[63] ATLAS Collaboration, *Search for top and bottom squarks from gluino pair production in final states with missing transverse energy and at least three b-jets with the ATLAS detector*, submitted to Eur. Phys. J. C , arXiv:1207.4686 [hep-ex].

## Auxiliary Plots

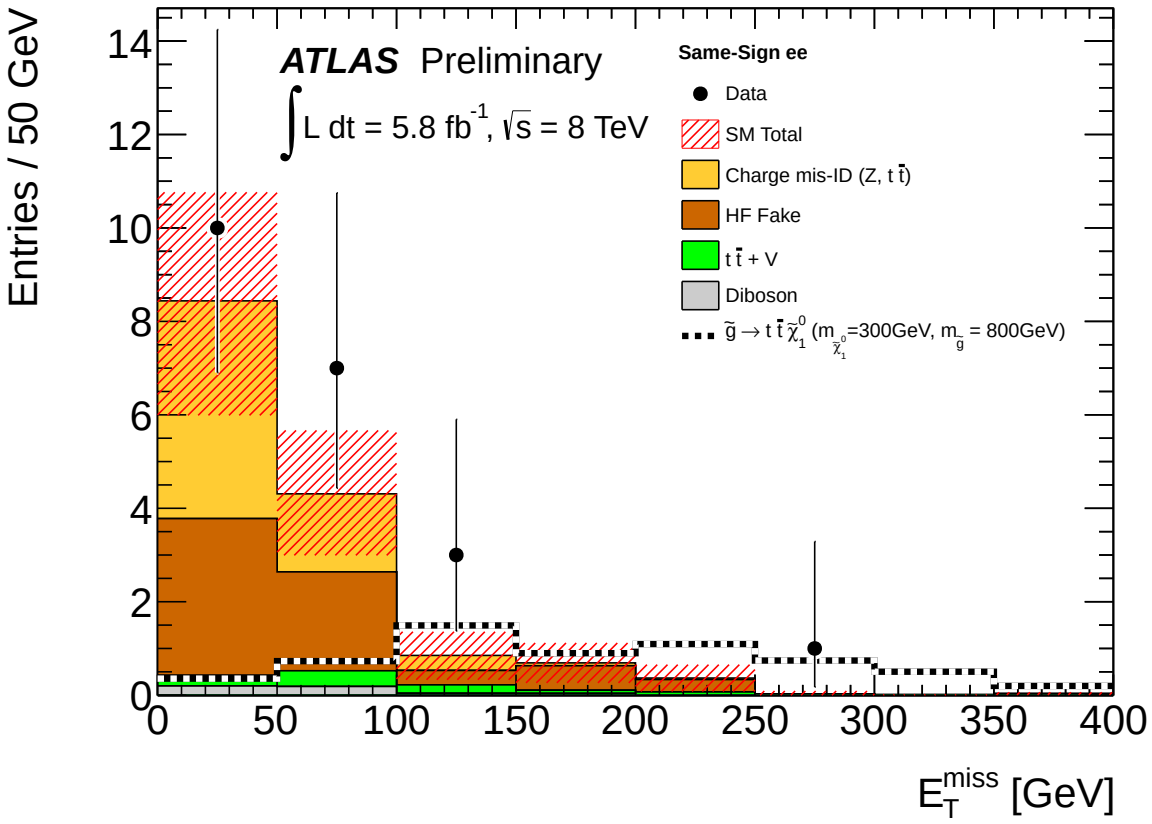


Figure 5: Distribution of $E_{\mathrm{T}}^{\mathrm{miss}}$ for *ee* events with the baseline selection. The data points are compared with the sum of the expected contribution from HF fakes, real SS dileptons from diboson and $t\bar{t} + V$ as well as charge mis-identification from $t\bar{t}$ or $Z$+jets events. The red-shaded error band around the expectation contains all statistical and systematical uncertainties of the background prediction.

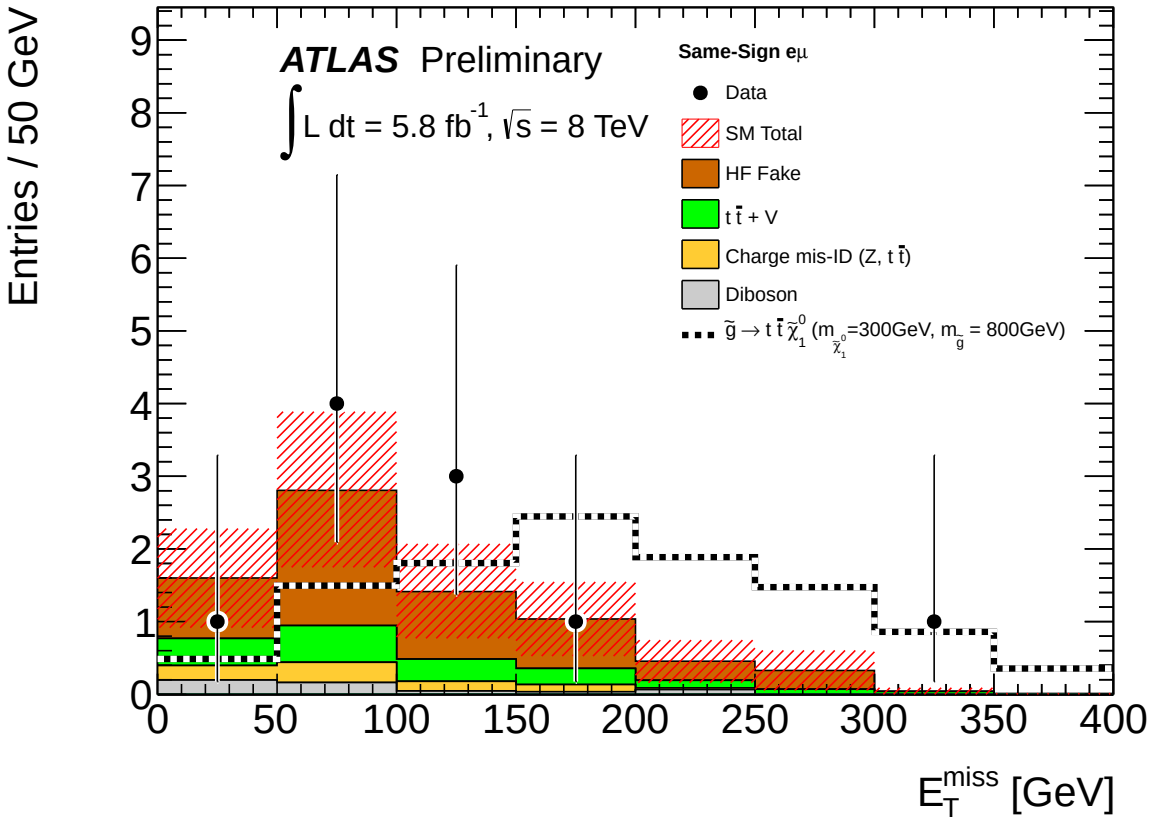


Figure 6: Distribution of $E_{\mathrm{T}}^{\mathrm{miss}}$ for $e\mu$ events with the baseline selection. The data points are compared with the sum of the expected contribution from HF fakes, real SS dileptons from diboson and $t\bar{t}+V$ as well as charge misidentification from $t\bar{t}$ or $Z$+jets events. The red-shaded error band around the expectation contains all statistical and systematical uncertainties of the background prediction.

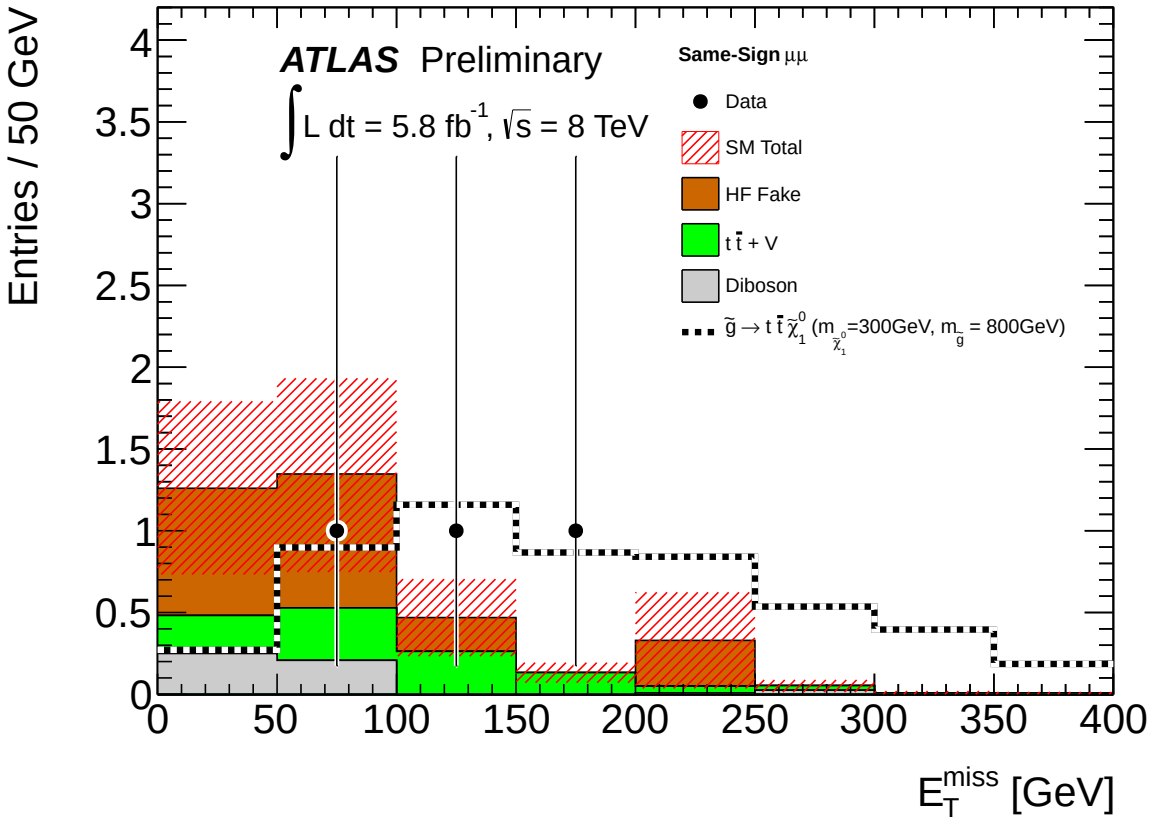


Figure 7: Distribution of $E_{\mathrm{T}}^{\mathrm{miss}}$ for $\mu\mu$ events with the baseline selection. The data points are compared with the sum of the expected contribution from HF fakes and real SS dileptons from diboson and $t\bar{t} + V$. Charge mis-identification is negligible for $\mu\mu$. The red-shaded error band around the expectation contains all statistical and systematical uncertainties of the background prediction.